# Lepton Flavor Violating $\tau^- \to \mu^- V^0$ Decays in the Two Higgs Doublet Model III

Wenjun Li*

*Department of Physics, Henan Normal University, XinXiang, Henan, 453007, P.R.China*

*Kavli Institute for Theoretical Physics China, CAS, Beijing 100190, China*

Yanqin Ma, Gongwei Liu, Wei Guo

*Department of Physics, Henan Normal University, XinXiang, Henan, 453007, P.R.China*



In this paper, the lepton flavor violating $\tau^- \to \mu^- V^0 (V^0 = \rho^0, \phi, \omega)$ decays are studied in the framework of the two Higgs doublet model(2HDM) III. We present a computation of the the $\gamma-$, $Z$ penguin and box diagrams contributions, and make an analysis of their impacts. Our results show that, among the $\gamma-$ penguins, the penguins with neutral Higgs in the loop are very larger than those with charged Higgs in the loop. We find that the model parameter $\lambda_{\tau\mu}$ is tightly constrained at the order of $O(10^{-3})$ and the branching ratios of these decays are available at the experiment measure. With the high luminosity, the B factories have considerable capability to find these LFV processes. On the other hand, these processes can also provide some valuable information to future research and furthermore present the reliable evidence to test the 2HDM III model.

PACS numbers: 13.35.Dx, 12.15.Mm, 12.60.-i

## I. INTRODUCTION

The flavor physics is always the hot subject in particle physics. Recently, with rapid development of neutrinos experiment[1], the lepton flavor violation(LFV) processes of charged-lepton sector have attracted many people's attention. In the standard model(SM), the LFV processes are forbidden. Hence, the LFV decays are expected to be a powerful probe to many extensions of the SM with new LFV source and/or new particles.

The LFV $\tau$ decays have become a seeking goal in experiment. Due to the comparability of $e^+e^- \to b\bar{b}$ and $e^+e^- \to \tau^-\tau^-$ cross section ($\sigma \sim 0.99nb$) around the $\Upsilon(4s)$ energy region, large events of $\tau$ leptons are available at BaBar and Belle ($\mathcal{L}_{BaBar}$ $470fb^{-1}, \mathcal{L}_{Belle}$ $710fb^{-1}$). And now the tau pairs production has attained the reach of $10^{-9}$. The tau factory has performed the experimental search for the tau radiative decays and $\tau \to 3l$ decays, as well as $\tau \to lV^0$ decays[2]. The current experimental upper limits of the $\tau^- \to \mu^-\rho^0(\phi, \omega)$ decays with $543fb^{-1}$

*Electronic address: liwj24@163.com

of data at Belle laboratory are [3]:

$$\mathcal{B}(\tau^- \to \mu^- \rho^0) < 6.8 \times 10^{-8}, \quad 90\% CL$$

$$\mathcal{B}(\tau^- \to \mu^- \phi) < 1.3 \times 10^{-7}, \quad 90\% CL$$

$$\mathcal{B}(\tau^- \to \mu^- \omega) < 8.9 \times 10^{-8}, \quad 90\% CL \tag{1}$$

There are also lots of theoretical researches on $\tau \to lV^0$ decays in many possible extensions of the SM. For example, Saha *et al.* have deliberated constraints on the parameters from $\tau \to l\rho^0(\phi, K^{*0}, \bar{K}^{*0})$ decays in RPV SUSY model[4]. Ilakovac *et al.* found only the ratios of $\tau^- \to e^-\rho^0(\phi, \pi^0)$ decays reach the order of $10^{-6}$ in models with heavy Dirac or Majorana neutrinos[5]. The case of $\tau \to lP(V^0)$ decays in topcolor model have been considered by Yue Chongxing *et al.*[6]. Such investigations also have been presented in MSSM and minimal susysemmetry $SO(10)$ models[7], a general unconstrained MSSM model[8] and two constrained MSSM seesaw models[9] as well.

In our previous work[10], we have studied the $\tau \to \mu P(P = \pi^0, \eta, \eta')$ decays in 2HDM model III. In this model, there exist flavor-changing neutral currents(FCNCs) at tree level. In order to satisfy the current experiment constrains, the tree-level FCNCs are suppressed in low-energy experiments for the first two generation fermions. While processes concerning with the third generation fermions would be larger. These FCNCs with neutral Higgs bosons mediated may produce sizable effects to the $\tau-\mu$ transition. The $\tau \to \mu P$ decays could yield one pseudoscalar meson from the vacuum state through the scalar and pseudoscalar currents. Hence, this type decay could occur at the tree level through the neutral Higgs bosons exchange. In this paper, we extend our discussion to the case of one vector meson in the hadronic final state. Different from pseudoscalar meson, the vector meson is only generated through vector currents and therefore receive no contributions of the neutral Higgs at tree level. So we consider the effects with Higgs bosons in the loop. There are the $\gamma-$, $Z$ penguin and the box diagrams for the $\tau \to \rho^0(\phi, \omega)$ decays. For the instance of vector meson $K^{*0}(\bar{K}^{*0})$, the LFV processes could occur at loop level likewise but the additional loop at the hadronic vertex would generate one suppressed factor. So these two decays are not discussed in this paper. Our results suggest that, in the $\gamma-$ penguins, the contributions of penguin with neutral Higgs bosons in the loop is greater than those of penguin with charged Higgs bosons in the loop. The model parameter $\lambda_{\tau\mu}$ is restrained at $O(10^{-3})$ and the decay branching ratios could as large as the current upper limits of $O(10^{-7})$. For $\tau^- \to \mu^- PP$ processes, we will make further study in our later work.

The paper is organized as follows: In section II, we make a brief introduction of the theoretical framework for the two-Higgs-doublet model III. In section III, we present the decay amplitudes and the numerical predictions for the branching ratios. Our conclusions are listed in the last section.

## II. THE TWO-HIGGS -DOUBLET MODEL III

As the simplest extension of the SM, the Two-Higgs-Doublet Model has an additional Higgs doublet. In order to ensure the forbidden FCNCs at tree level, it requires either the same doublet couple to the $u$-type and $d$-type quarks(2HDM I) or one scalar doublet couple to the $u$-type quarks and the other to $d$-type quarks(2HDM II). While in the 2HDM III[11, 12], two Higgs doublets could couple to the $u$-type and $d$-type quarks simultaneously. Particularly, without an *ad hoc* discrete symmetry exerted, this model permits flavor changing neutral currents occur at the tree level.

The Yukawa Lagrangian is generally expressed as the following form:

$$\mathcal{L}_Y = \eta^U_{ij}\bar{Q}_{i,L}\tilde{H}_1 U_{j,R} + \eta^D_{ij}\bar{Q}_{i,L}H_1 D_{j,R} + \xi^U_{ij}\bar{Q}_{i,L}\tilde{H}_2 U_{j,R} + \xi^D_{ij}\bar{Q}_{i,L}H_2 D_{j,R} \; + \; h.c., \tag{2}$$

where $H_i (i = 1, 2)$ are the two Higgs doublets. $Q_{i,L}$ is the left-handed fermion doublet, $U_{j,R}$ and $D_{j,R}$ are the right-handed singlets, respectively. These $Q_{i,L}, U_{j,R}$ and $D_{j,R}$ are weak eigenstates, which can be rotated into mass eigenstates. While $\eta^{U,D}$ and $\xi^{U,D}$ are the non-diagonal matrices of the Yukawa couplings.

We can conveniently choose a suitable basis to denote $H_1$ and $H_2$ as:

$$H_1 = \frac{1}{\sqrt{2}}\left[\begin{pmatrix} 0 \\ v+\phi^0_1 \end{pmatrix} + \begin{pmatrix} \sqrt{2}\,G^+ \\ iG^0 \end{pmatrix}\right], \quad H_2 = \frac{1}{\sqrt{2}}\begin{pmatrix} \sqrt{2}\,H^+ \\ \phi^0_2 + iA^0 \end{pmatrix}, \tag{3}$$

where $G^{0,\pm}$ are the Goldstone bosons, $H^\pm$ and $A^0$ are the physical charged-Higgs boson and CP-odd neutral Higgs boson, respectively. Its virtue is the first doublet $H_1$ corresponds to the scalar doublet of the SM while the new Higgs fields arise from the second doublet $H_2$.

The CP-even neutral Higgs boson mass eigenstates $H^0$ and $h^0$ are linear combinations of $\phi^0_1$ and $\phi^0_2$ in Eq.(3),

$$H^0 \;=\; \phi^0_1\cos\alpha + \phi^0_2\sin\alpha, \;\; h^0 = -\phi^0_1\sin\alpha + \phi^0_2\cos\alpha, \tag{4}$$

where $\alpha$ is the mixing angle.

After diagonalizing the mass matrix of the fermion fields, the Yukawa Lagrangian becomes[13]

$$\begin{aligned}
L_Y \;=\; & -\overline{U}M_U U - \overline{D}M_D D + \frac{i}{v}\chi^0\left(\overline{U}M_U\gamma_5 U - \overline{D}M_D\gamma_5 D\right) \\
+ \; & \frac{\sqrt{2}}{v}\chi^-\overline{D}V^\dagger_{CKM}\left[M_U R - M_D L\right]U - \frac{\sqrt{2}}{v}\chi^+\overline{U}V_{CKM}\left[M_D R - M_U L\right]D \\
+ \; & \frac{iA^0}{\sqrt{2}}\left\{\overline{U}\left[\widehat{\xi}^U R - \widehat{\xi}^{U\dagger}L\right]U + \overline{D}\left[\widehat{\xi}^{D\dagger}L - \widehat{\xi}^D R\right]D\right\} \\
- \; & \frac{H^0}{\sqrt{2}}\overline{U}\left\{\frac{\sqrt{2}}{v}M_U\cos\alpha + \left[\widehat{\xi}^U R + \widehat{\xi}^{U\dagger}L\right]\sin\alpha\right\}U - \frac{H^0}{\sqrt{2}}\overline{D}\left\{\frac{\sqrt{2}}{v}M_D\cos\alpha + \left[\widehat{\xi}^D R + \widehat{\xi}^{D\dagger}L\right]\sin\alpha\right\}D \\
- \; & \frac{h^0}{\sqrt{2}}\overline{U}\left\{-\frac{\sqrt{2}}{v}M_U\sin\alpha + \left[\widehat{\xi}^U R + \widehat{\xi}^{U\dagger}L\right]\cos\alpha\right\}U - \frac{h^0}{\sqrt{2}}\overline{D}\left\{\frac{\sqrt{2}}{v}M_D\sin\alpha + \left[\widehat{\xi}^D R + \widehat{\xi}^{D\dagger}L\right]\cos\alpha\right\}D \\
- \; & H^+\overline{U}\left[V_{CKM}\widehat{\xi}^D R - \widehat{\xi}^{U\dagger}V_{CKM}L\right]D - H^-\overline{D}\left[\widehat{\xi}^{D\dagger}V^\dagger_{CKM}L - V^\dagger_{CKM}\widehat{\xi}^U R\right]U
\end{aligned} \tag{5}$$

where U and D now are the fermion mass eigenstates and

$$\hat{\eta}^{U,D} = (V_L^{U,D})^{-1} \cdot \eta^{U,D} \cdot V_R^{U,D} = \frac{\sqrt{2}}{v} M^{U,D} (M_{ij}^{U,D} = \delta_{ij} m_j^{U,D}), \tag{6}$$

$$\hat{\xi}^{U,D} = (V_L^{U,D})^{-1} \cdot \xi^{U,D} \cdot V_R^{U,D}, \tag{7}$$

where $V_{L,R}^{U,D}$ are the rotation matrices acting on up and down-type quarks, with left and right chiralities respectively. Thus $V_{CKM} = (V_L^U)^\dagger V_L^D$ is the usual Cabibbo-Kobayashi-Maskawa (CKM) matrix. In general, the matrices $\hat{\eta}^{U,D}$ of Eq.(6) are diagonal, while the matrices $\hat{\xi}^{U,D}$ are non-diagonal which could induce scalar-mediated FCNC. Seen from Eq.(5), the coupling of neutral Higgs bosons to the fermions could generate FCNC parts. For the arbitrariness of definition for $\xi_{ij}^{U,D}$ couplings, we can adopt the rotated couplings expressed $\xi^{U,D}$ in stead of $\hat{\xi}^{U,D}$ hereafter.

In this work, we use the Cheng-Sher ansatz[11]

$$\xi_{ij}^{U,D} = \lambda_{ij} \frac{\sqrt{m_i m_j}}{v} \tag{8}$$

which ensures that the FCNCs within the first two generations are naturally suppressed by small fermions masses. This ansatz suggests that LFV couplings involving the electron are suppressed, while LFV transitions involving muon and tau are much less suppressed and may lead to some loop effects which are promising to be tested by the future B factory experiments. In Eq.(8), the parameter $\lambda_{ij}$ is complex and $i, j$ are the generation indexes. In this study, we shall discuss the phenomenological applications of the type III 2HDM.

## III. THE DISCUSSION FOR $\tau^- \to \mu^- V^0$ DECAYS

As we have mentioned above, one vector meson could not be generated from the vacuum state through the scalar and/or pseudoscalar currents. In 2HDM model III, the neutral Higgs bosons mediated tree and penguin diagrams have no contributions to $\tau^- \to \mu^- V^0$ processes. Accordingly, their decay amplitudes acquire contributions from the $\gamma-, Z-$ penguin and box diagrams. Comparing to the $\tau \to \mu P$decays, in addition to neutral Higgs bosons, the penguin with charged Higgs bosons in the loop also contribute to these decays. We will make a detail analysis of their effects in the later paragraphs. The penguin diagrams at the quark level pertinent to these decays are list in Fig.1.

The amplitudes could be factorized into leptonic vertex corrections and hadronic parts described with hadronic matrix elements. In dealing with hadronic matrix elements, we take the generalized factorization approach and write the hadronic matrix elements as $< V|\bar{q}\gamma_\mu q|0 >= -m_V f_V \varepsilon_\mu^*$ with the decay constant $f_V$. The quark contents of $\rho^0$ meson are chosen as $\rho^0 = \frac{1}{\sqrt{2}}(-u\bar{u} + d\bar{d})$. For the vector $\phi - \omega$ meson system, we employ the ideal mixing scheme between $\phi(1020)$ and $\omega(782)$ which is supported by existing data: $\phi = -s\bar{s}, \omega = \frac{1}{\sqrt{2}}(u\bar{u} + d\bar{d})$[14]. Then,

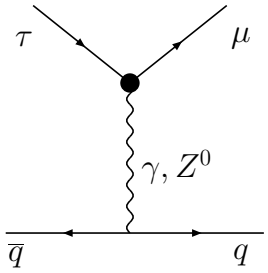


FIG. 1: The $\gamma$ and $Z^0$ penguin diagrams for $\tau^- \to \mu^- q\bar{q}$ decay, where the neutral and charged Higgs bosons are in the loop.

the total amplitudes could be expressed as:

$$\begin{aligned}
\mathcal{M}(\tau^- \to \mu^- V^0) &= \mathcal{M}_\gamma + \mathcal{M}_Z + \mathcal{M}_{box} \\
\mathcal{M}_\gamma(\tau^- \to \mu^- V^0) &= \frac{i\alpha_w^2 S_w^2}{2m_w^2} \cdot \bar{\mu} \cdot [F1_\gamma \cdot L + F2_\gamma \cdot R + F3_\gamma \cdot \gamma_\rho L + F4_\gamma \cdot \gamma_\rho R] \cdot \tau \\
&\quad \otimes \langle V^0 | \frac{2}{3}\bar{u}\gamma^\rho u - \frac{1}{3}\bar{d}\gamma^\rho d - \frac{1}{3}\bar{s}\gamma^\rho s|0\rangle \\
\mathcal{M}_Z &= \frac{i\alpha_w^2}{8m_W^4} \cdot \bar{\mu} \cdot \Big[F_1^z \cdot L + F_2^z \cdot R + F_3^z \cdot \gamma_\rho L + F_4^z \cdot \gamma_\rho R] \cdot \tau \\
&\quad \otimes \langle V^0 | g_V^u(\bar{u}\gamma^\rho u) - g_V^d(\bar{d}\gamma^\rho d) - g_V^s(\bar{s}\gamma^\rho s)|0\rangle \\
\mathcal{M}_{box} &= \frac{i\alpha_w^2}{m_W^4} \cdot \bar{\mu} \cdot \Big[F_1^{box} \cdot L + F_2^{box} \cdot R + F_3^{box} \cdot \gamma_\rho L + F_4^{box} \cdot \gamma_\rho R + F_5^{box} \cdot i\sigma_{\rho\lambda} L + F_6^{box} \cdot i\sigma_{\rho\lambda} R\Big] \cdot \tau \\
&\quad \otimes \langle V^0 | \bar{u}\gamma^\rho u - \bar{d}\gamma^\rho d - \bar{s}\gamma^\rho s|\rangle
\end{aligned} \tag{9}$$

where $\mathcal{M}_\gamma, \mathcal{M}_Z$ and $\mathcal{M}_{box}$ are the amplitudes of the $\gamma-$ penguin, Z penguin and box diagrams. The relevant auxiliary functions are listed in Appendix.

In our calculation, the input parameters are the Higgs masses, mixing angle $\alpha$, $|\lambda_{ij}|$ and their phase angles $\theta_{ij}$. Given the constraints from the current experiment permits and theoretical considerations[10, 15, 16, 17, 18, 19, 20], we assume

$$\begin{aligned}
m_{H^\pm} &= 200GeV,\ m_{H^0} = 160GeV,\ m_{h^0} = 115GeV,\ m_{A^0} = 120GeV,\ \alpha = \pi/4, \\
|\lambda_{uu}| &= 150,\ |\lambda_{dd}| = 120,\ |\lambda_{\tau\tau}| = 10,\ |\lambda_{tt}| = |\lambda_{tc}| = |\lambda_{ut}| = 0.03, \\
|\lambda_{ss}| &= |\lambda_{bb}| = |\lambda_{db}| = |\lambda_{bs}| = 100,\ \theta = \pi/4,
\end{aligned} \tag{10}$$

where the Higgs masses satisfy the relation $115GeV \leq m_{h^0} < m_{A^0} < m_{H^0} \leq 200GeV$[15, 16, 17], and the absolute value of $\lambda_{tt} \cdot \lambda_{bb}$ is approximate to three[17, 18].

Using the above parameters, we could get the contributions of three diagrams to these decays. As we expected, the contributions of box diagrams are $O(10^{-25})$ order or so which are very smaller than those of $\gamma-$ and $Z-$ penguins. Hence, we neglect the box diagrams contributions. We have studied the relation of branching ratio and

TABLE I: Constraints on the $\lambda_{\tau\mu}$ from $\tau^- \to \mu^-\rho^0(\phi,\omega)$ decays in the 2HDM III.

| Decay modes | Bounds on $\lambda_{\tau\mu}$ | Previous Bounds |
|---|---|---|
| $\tau \to \mu\rho^0$ | $\leq 1.26 \times 10^{-3}$ | $\lambda_{\tau\mu} \sim O(1)$ [21] |
| $\tau \to \mu\phi$ | $\leq 2.45 \times 10^{-3}$ | $\lambda_{\tau\mu} \sim O(10)$ [10, 22, 23], $\lambda_{\tau\mu} \sim O(10) - O(10^2)$ [16] |
| $\tau \to \mu\omega$ | $\leq 1.48 \times 10^{-3}$ | $\lambda_{\tau\mu} \sim O(10^2) - O(10^3)$ [24] |

$\lambda_{\tau\mu}$. The computation indicate that the variation of $\theta_{\tau\mu}$, the phase angle of parameters $\lambda_{\tau\mu}$, does almost not affect the values of branching ratios. So we take $\theta_{\tau\mu} = \pi/4$ as literatures do.

The Fig.2 gives the total penguin contributions denoted by the solid line. We denote the $\gamma-$ penguin and the $Z-$ penguin contributions by the dash line and the dot line, respectively. Due to the suppressed factor $O(1/m_Z^2)$ from the Z propagator, the $Z$ penguin contributions are supposed to be lower than those of the $\gamma-$ penguin. These decay amplitudes have common leptonic parts, so the differences of decay amplitudes mainly come from the hadronic parts. For the similar contents of $\rho^0$ and $\omega$, the curves of $\tau^- \to \mu^-\rho^0$ and $\tau^- \to \mu^-\omega$ decays display similar trend, namely, their $Z$ penguin contributions are lower one order than those of their $\gamma-$ penguin. However, for $\tau^- \to \mu^-\phi$ decay, the magnitudes of $Z$ penguin are close to the $\gamma-$ penguin contributions.

The relations of ratios versus $|\lambda_{\tau\mu}|$ are also presented in Fig.2, where the horizon lines denote the experimental upper limits. Evidently, one can see from Fig.2 that these branching ratios rise with the increase of $|\lambda_{\tau\mu}|$. We have got the constraints on $|\lambda_{\tau\mu}|$ from the experimental data, which are list in Table.I. It is obviously that the parameter $|\lambda_{\tau\mu}|$ is restrained at the order of $O(10^{-3})$. The $|\lambda_{\tau\mu}|$ constraints for $\tau^- \to \mu^-\rho^0(\omega)$ are little severe than that of $\tau^- \to \mu^-\phi$ decay. The bounds of $|\lambda_{\tau\mu}|$ from different phenomenological considerations [10, 16, 21, 22, 23, 24] are demonstrated in Tab.I, too. Comparing the values of $\lambda_{\tau\mu}$ in Tab.I, one can see that our constraint is stringenter than the limits in literatures.

Now we illustrate the contributions of $\gamma-$ penguin with neutral and charged Higgs bosons in the loop. In Fig.3, the solid line denotes the $\gamma-$ penguin contributions, the dash line and the dot line denote the contributions of $\gamma-$ penguin with neutral Higgs bosons in the loop and those of $\gamma-$ penguin with charged Higgs bosons in the loop, respectively. Apparently, the contributions of $\gamma-$ penguin with neutral Higgs in the loop are quite higher by nearly four order magnitudes than those of $\gamma-$ penguin with charged Higgs in the loop. And the dot line and the solid line coincide with each other for three decays. As a result, the contributions of $\gamma-$ penguin with neutral Higgs in the loop are dominated one.

The contributions of $Z$ penguin with charged and neutral Higgs bosons in the loop are demonstrated in figure 4. The solid line denotes the $Z$ penguins contributions, the dash line and the dot line denote the contributions

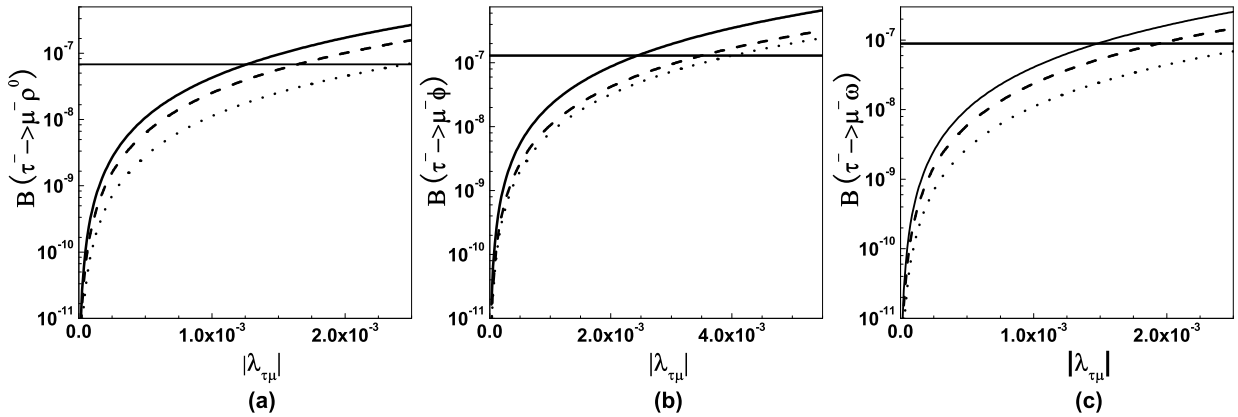


FIG. 2: The branching ratios versus model parameter $|\lambda_{\tau\mu}|$ with $\theta_{\tau\mu} = \pi/4$, (a) for $\tau^- \to \mu^-\rho^0$ decay, (b) for $\tau^- \to \mu^-\phi$ decay, and (c) for $\tau^- \to \mu^-\omega$ decay. The solid line denotes the total contributions; the dash line and the dot line denote the $\gamma-$ and Z penguin contributions, respectively. The horizontal lines are the experimental upper limits.

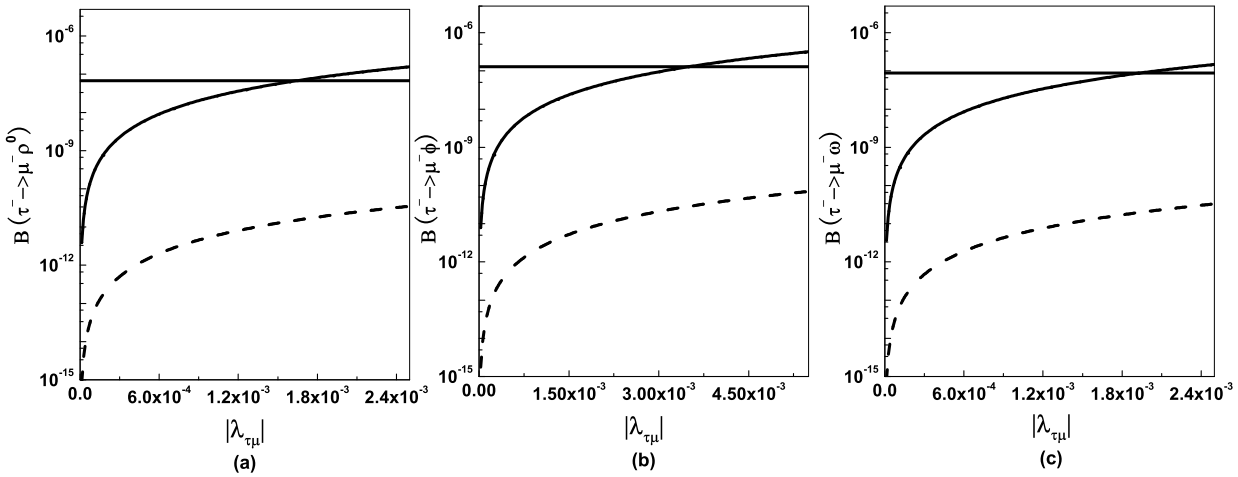


FIG. 3: The branching ratios versus model parameter $|\lambda_{\tau\mu}|$ with $\theta_{\tau\mu} = \pi/4$, (a) for $\tau^- \to \mu^-\rho^0$ decay (b) for $\tau^- \to \mu^-\phi$ decay, and (c) for $\tau^- \to \mu^-\omega$ decay. The solid line denotes the $\gamma$ penguin contributions; the dash line and the dot line denote the contributions of $\gamma-$ penguin with neutral Higgs bosons in the loop and those of $\gamma-$ penguin with charged Higgs bosons in the loop, respectively.

of $Z$ penguin with charged Higgs bosons in the loop and those of $Z$ penguin with neutral Higgs bosons in the loop, respectively. Unlike the case of $\gamma$ penguin, the contributions of $Z$ penguin with neutral Higgs in the loop are rather smaller by nearly eight order magnitudes than those of $Z$ penguin with charged Higgs in the loop. So the contributions of $Z$ penguin with neutral Higgs in the loop are subordinate one. In a word, the $\gamma-$ penguin with neutral Higgs in the loop plays a main role in these decays.

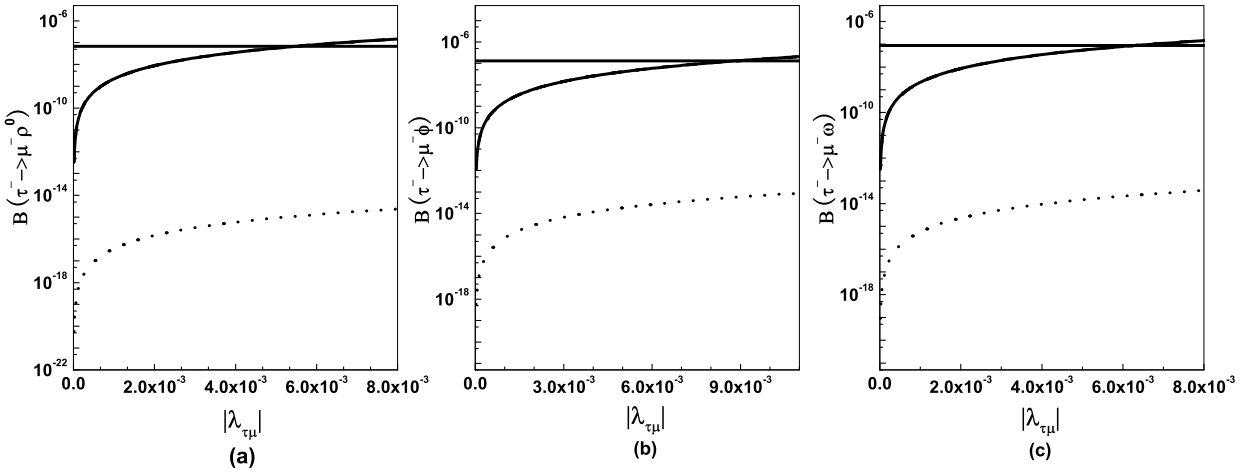


FIG. 4: The branching ratios versus model parameter $|\lambda_{\tau\mu}|$ with $\theta_{\tau\mu} = \pi/4$, (a) for $\tau^- \to \mu^-\rho^0$ decay (b) for $\tau^- \to \mu^-\phi$ decay, and (c) for $\tau^- \to \mu^-\omega$ decay. The solid line denotes the Z penguin contributions; the dash line and the dot line denote the contributions of $Z$ penguin with charged Higgs bosons in the loop and those of $Z$ penguin with neutral Higgs bosons in the loop, respectively

## IV. CONCLUSION

In summary, we have calculated the branching ratios of $\tau^- \to \mu^-\rho^0(\phi,\omega)$ decays in the model III 2HDM. Comparing to the $\tau^- \to \mu^- P$ decays, besides the neutral higgs bosons in the loop, an additional charged Higgs boson in the loop offer contributions to $\tau^- \to \mu^- V^0$ decays. The impacts of the $\gamma-$ penguin, $Z-$ penguin and those of two types Higgs in loop are formulated. It is concluded that the $\gamma-$ penguin with neutral Higgs bosons in loop are dominated in the $\gamma-$ penguin, while the $Z-$ penguin with charged Higgs bosons in loop mainly contributes to the $Z-$ penguins. Our work suggests that the parameter $|\lambda_{\tau\mu}|$ is constrained at the order of $O(10^{-3})$. And in the rational parameters space, the $Br(\tau^- \to \mu^- V^0)$ can reach the experimental values. With the experiment luminosity increasing, these LFV decays are available to the collider's measure capability. Our study is hoped to supply good information for the future experiment and explore the structure of the 2HDM III model.

## Appendix

For simplicity, we only list the amplitude of $\gamma-$ penguin.

The amplitude of $\gamma-$ penguin diagrams is

$$\begin{aligned}\mathcal{M}_\gamma(\tau^- \to \mu^- V^0) &= \frac{i\alpha_w^2 S_w^2}{2m_w^2}\cdot\bar{\mu}\cdot[F1_\gamma\cdot L + F2_\gamma\cdot R + F3_\gamma\cdot\gamma_\rho L + F4_\gamma\cdot\gamma_\rho R]\cdot\tau \\ &\otimes\langle V^0|\frac{2}{3}\bar{u}\gamma^\rho u - \frac{1}{3}\bar{d}\gamma^\rho d - \frac{1}{3}\bar{s}\gamma^\rho s|0\rangle. \end{aligned} \tag{11}$$

Where the auxiliary functions $F_\gamma$ are written as:

$$
\begin{aligned}
F1_\gamma &= \frac{m_\tau\sqrt{m_\tau m_\mu}\cdot}{k^2}\cdot\int_0^1 dx\int_0^{1-x} dy\left\{\left(-\frac{m_\tau\lambda^*_{\tau\mu}\lambda_{\tau\tau}\cdot x}{S_c(x,y,m^2_{H^-},x_{tc})}+\frac{m_\tau\lambda^*_{\tau\mu}}{2}\sum_i J_i\times x\right)\cdot p_1^\rho\right.\\
&\left.+\left(-\frac{m_\tau\cdot\lambda^*_{\tau\mu}\lambda_{\tau\tau}\cdot x}{S_c(x,y,m^2_{H^-},x_{tc})}+\frac{1}{2}\sum_i K_i\times y\right)\cdot p_2^\rho\right\}, \qquad (12)\\
F2_\gamma &= \frac{m_\tau\sqrt{m_\tau m_\mu}}{k^2}\cdot\int_0^1 dx\int_0^{1-x} dy\left\{\left(-\frac{m_\mu\cdot\lambda^*_{\tau\mu}\lambda_{\tau\tau}\cdot y}{S_c(x,y,m^2_{H^-},x_{tc})}+\frac{m_\tau\cdot\lambda_{\tau\mu}}{2}\cdot\sum_i J_i^*\times x\right)\cdot p_1^\rho\right.\\
&\left.+\left(-\frac{m_\mu\cdot\lambda^*_{\tau\mu}\lambda_{\tau\tau}\cdot y}{S_c(x,y,m^2_{H^-},x_{tc})}+\frac{1}{2}\cdot\sum_i K_i^*\times y\right)\cdot p_2^\rho\right\}, \qquad (13)
\end{aligned}
$$

$$
F3_\gamma = \frac{m_\tau\sqrt{m_\tau m_\mu}}{k^2}\cdot\left\{\frac{1}{(m_\tau^2-m_\mu^2)}\cdot\int_0^1 dx\left[m_\mu\cdot\lambda^*_{\tau\mu}\lambda_{\tau\tau}(x-1)\ln\frac{S_a(x,x_{tc})}{S_b(x)}+\frac{1}{2}M_i\right]+N+\int_0^1 dx\int_0^{1-x} dyQ_i\right\}, \qquad (14)
$$

$$
\begin{aligned}
F4_\gamma &= \frac{m_\tau\sqrt{m_\tau m_\mu}}{k^2}\cdot\left\{\frac{1}{(m_\tau^2-m_\mu^2)}\cdot\int_0^1 dx\left[\lambda^*_{\tau\mu}\lambda_{\tau\tau}(x-1)\cdot\left(m_\tau^2\ln S_a(x,x_{tc})-m_\mu^2\ln S_b(x)\right)+\frac{1}{2}M_i^*\right]+N^*\right.\\
&\left.+\int_0^1 dx\int_0^{1-x} dy[\ln\frac{S_c(x,y,m^2_{H^-},x_{tc})}{\mu^2}+Q_i^*]\right\}. \qquad (15)
\end{aligned}
$$

The followings are expressions of $J_i, K_i, M_i, N$ and $Q_i$.

$$
\begin{aligned}
J_{H^0} &= \frac{\omega_s}{S_c^{H^0}(x,y,m^2_{H^0},x^{H^0}_{tn})},\quad J_{h^0}=\frac{\upsilon_s}{S_c^{h^0}(x,y,m^2_{h^0},x^{h^0}_{tn})},\quad J_{A^0}=\frac{2iIm\lambda_{\tau\tau}}{S_c^{A^0}(x,y,m^2_{A^0},x^{A^0}_{tn})},\\
K_{H^0} &= (m_\tau\lambda^*_{\tau\mu}+m_\mu\lambda_{\tau\mu})\times J^*_{H^0},\quad K_{h^0}=(m_\tau\lambda^*_{\tau\mu}+m_\mu\lambda_{\tau\mu})\times J^*_{h^0},\quad K_{A^0}=\frac{\lambda^*_{\tau\tau}(m_\mu\lambda_{\tau\mu}-m_\tau\lambda^*_{\tau\mu})}{S_c^{A^0}(x,y,m^2_{A^0},x^{A^0}_{tn})}\\
M_{H^0} &= \Big[[x(m_\tau^2\omega^*\lambda_{\tau\mu}+m_\tau m_\mu\omega\lambda^*_{\tau\mu})-\omega_s(m_\tau^2\lambda_{\tau\mu}+m_\tau m_\mu\lambda^*_{\tau\mu})]\ln S_a^{H^0}(x,x^{H^0}_{tn})\\
&\quad -[x(m_\mu^2\omega^*\lambda_{\tau\mu}+m_\tau m_\mu\omega\lambda^*_{\tau\mu})-(m_\mu^2\omega^*+m_\tau^2\omega)\lambda_{\tau\mu}-m_\tau m_\mu\omega_s\lambda^*_{\tau\mu}]\ln S_b^{H^0}(x)\Big]\\
Q_{H^0} &= \int_0^1 dx\int_0^{1-x} dy\Big(\omega^*\lambda_{\tau\mu}[\ln\frac{S_c(x,y,m^2_{H^-},x_{tc})}{\mu^2}+\frac{m_\tau^2(x^2-x-1)-m_\mu^2y}{S_c^{H^0}(x,y,m^2_{H^0},x^{H^0}_{tn})}]\\
&\quad +\frac{m_\tau m_\mu\lambda^*_{\tau\mu}[(x+y)\omega-\omega_s]-m_\tau^2\omega\lambda_{\tau\mu}}{S_c^{H^0}(x,y,m^2_{H^0},x^{H^0}_{tn})}\Big)\\
M_{h^0} &= [x(m_\tau^2\upsilon^*\lambda_{\tau\mu}+m_\tau m_\mu\upsilon\lambda^*_{\tau\mu})-\upsilon_s(m_\tau^2\lambda_{\tau\mu}+m_\tau m_\mu\lambda^*_{\tau\mu})]\ln S_a^{h^0}(x,x^{h^0}_{tn})\\
&\quad -[x(m_\mu^2\upsilon^*\lambda_{\tau\mu}+m_\tau m_\mu\upsilon\lambda^*_{\tau\mu})-(m_\mu^2\upsilon^*+m_\tau^2\upsilon)\lambda_{\tau\mu}-m_\tau m_\mu\upsilon_s\lambda^*_{\tau\mu}]\ln S_b^{h^0}(x)\Big]\\
Q_{h^0} &= \Big([\ln\frac{S_c(x,y,m^2_{H^-},x_{tc})}{\mu^2}+\frac{m_\tau^2(x^2-x-1)-m_\mu^2y}{S_c^{h^0}(x,y,m^2_{h^0},x^{h^0}_{tn})}]\upsilon^*\lambda_{\tau\mu}\\
&\quad +\frac{m_\tau m_\mu\lambda^*_{\tau\mu}[(x+y)\upsilon-\upsilon_s]-m_\tau^2\upsilon\lambda_{\tau\mu}}{S_c^{h^0}(x,y,m^2_{h^0},x^{h^0}_{tn})}\Big)\\
M_{A^0} &= \Big[[x(m_\tau^2\lambda^*_{\tau\tau}\lambda_{\tau\mu}+m_\tau m_\mu\lambda_{\tau\tau}\lambda^*_{\tau\mu})-2iIm\lambda_{\tau\tau}(m_\tau m_\mu\lambda^*_{\tau\mu}-m_\tau^2\lambda_{\tau\mu})]\ln S_a^{A^0}(x,x^{A^0}_{tn})\\
&\quad -[x(m_\mu^2\lambda^*_{\tau\tau}\lambda_{\tau\mu}+m_\tau m_\mu\lambda_{\tau\tau}\lambda^*_{\tau\mu})-(m_\mu^2\lambda^*_{\tau\tau}-m_\tau^2\lambda_{\tau\tau})\lambda_{\tau\mu}-2im_\tau m_\mu\lambda^*_{\tau\mu}Im\lambda_{\tau\tau}]\ln S_b^{A^0}(x)\Big]\\
Q_{A^0} &= \Big([\ln\frac{S_c^{A^0}(x,y,m^2_{A^0},x^{A^0}_{tn})}{\mu^2}+\frac{m_\tau^2(x^2-x-1)-m_\mu^2y}{S_c^{A^0}(x,y,m^2_{A^0},x^{A^0}_{tn})}]\lambda^*_{\tau\tau}\lambda_{\tau\mu}\\
&\quad +\frac{m_\tau^2\lambda_{\tau\tau}\lambda_{\tau\mu}+m_\tau m_\mu\lambda^*_{\tau\mu}[(x+y)\lambda_{\tau\tau}-2iIm\lambda_{\tau\tau}]}{S_c^{A^0}(x,y,m^2_{A^0},x^{A^0}_{tn})}\Big)
\end{aligned}
$$

$$
\begin{aligned}
N &= \frac{1}{2}\lambda_{\tau\mu}(\omega^* + \upsilon^* + \lambda^*_{\tau\tau}) \\
\omega &= (\lambda_{\tau\tau}\sin^2\alpha + \sin\alpha\cos\alpha), \quad \upsilon = (\lambda_{\tau\tau}\cos^2\alpha - \sin\alpha\cos\alpha) \\
\omega_s &= 2\sin^2\alpha Re\lambda_{\tau\tau} + \cos 2\alpha, \quad \upsilon_s = 2\cos^2\alpha Re\lambda_{\tau\tau} - \cos 2\alpha
\end{aligned}
$$

The integrate function expressions are :

$$
\begin{aligned}
S_a(x, x_{tc}) &= (x-1)(x_{tc}x - 1), \quad S_b(x) = 1 - x, \;\; S_c(x, y, m^2_{H^-}, x_{tc}) = m^2_{H^-}[x + (x^2 - x + y)x_{tc}], \;\; x_{tc} = \frac{m^2_\tau}{m^2_{H^-}}, \\
S^i_a(x, x^i_{tn}) &= (x-1)(x^i_{tn}x - 1) \quad S^i_b(x) = S_b(x), \;\; S^i_c(x, y, m^2_i, x^i_{tn}) = m^2_i[y + x + x^i_{tn}x(x-1)], \;\; x^i_{tn} = \frac{m^2_\tau}{m^2_i} \qquad (16)
\end{aligned}
$$


**Acknowledgments**

I thank Prof.Chaoshang Huang for discussion. The work is supported by National Science Foundation under contract No.10547110, Henan Educational Committee Foundation under contract No.2007140007, the Project of Knowledge Innovation Program (PKIP) of Chinese Academy of Sciences under Grant No.KJCX2.YW.W10.



[1] Y. Fukuda, *et al.*, Super-Kmiokande Collaboration, Phys. Lett. **B433**, 9(1998); *ibid.* Phys. Lett. **B436**, 33(1998); *ibid.* Phys. Rev. Lett. **81**, 1562(1998).

[2] Y. Yusa,*et al.*, Belle Collaboration, Phys. Lett. **B640**:138-144(2006), [arXiv:hep-ph/0603036]; B. Aubert, *et al.*,BaBar Collaboration, Phys. Rev. Lett.**100**, 071802(2008), [arXiv:hep-ex/07110980].

[3] Y. Nishio, *et al.*, Belle Collaboration, Phys. Lett. **B664**:35-40(2008), [arXiv:hep-ph/0801.2475].

[4] J.P. Saha and A. Kundu, Phys. Rev. **D66**, 054021(2002).

[5] A. Ilakovac, Bernd A. Kniehl, Apostolos Pilaftsis, Phys.Rev. **D52**, 3993(1995)

[6] Chong-Xing Yue, Li-Hong Wang, Wei Ma, Phys. Rev. **D74**, 115018(2006).

[7] T.Fukuyama, A.Ilakovac and T.Kikuchi, Eur. Phys. J.**C56**:125-146(2008), [arXiv:hep-ph/0506295].

[8] A. Brignole and A. Rossi, Nucl. Phys. **B701**, 3(2004).

[9] E. Arganda, *et al.*, JHEP **0806**, 079(2008), [arXiv:hep-ph/0803.2639v3].

[10] Wenjun Li, Yadong Yang and Xiangdan Zhang, Phys. Rev. **D73**, 073005(2006).

[11] T. P. Cheng and M. Sher, Phys. Rev. **D35**, 3484(1987).

[12] W.S. Hou, Phys. Lett. **B296**, 179(1992); A. Antaramian, L.J. Hall, and A. Rasin, Phys. Rev. Lett. **69**, 1871(1992); L.J. Hall and S. Weinberg, Phys. Rev. **D48**, 979 (1993); M.J. Savage, Phys. Lett. **B266**, 135(1991); L. Wolfenstein and Y.L. Wu, Phys. Rev. Lett. bf 73, 2809(1994).

[13] David Bowser-Chao, King-man Cheung, Wai-Yee Keung, Phys. Rev. **D59**, 115006(1999), [arXiv:hep-ph/9811235].

[14] Xin-fen Chen, Dong-qin Guo, and Zhen-jun Xiao, [arXiv:hep-ph/0701146].

[15] Yuan-Ben Dai, *et al.*,Phys.Rev.**D67**, 096007(2003).

[16] Rodolfo A. Diaz, *et al.*, Phys. Rev. **D67**, 075011(2003).

[17] Chao-Shang Huang, Jian-Tao Li, Int. J. Mod. Phys. **A20**, 161(2005), [arXiv:hep-ph/0405294].

[18] Y.L.Wu. and C. Zhuang, [arXiv:hep-ph/0701072].

[19] D. Atwood, L. Reina, and A. Soni, Phys. Rev. Lett. **75**, 3800(1995); Phys. Rev. **D53**, 1199(1996); Phys. Rev. **D55**, 3156(1997).

[20] R. Martinez, J.-Alexis Rodriguez, M. Rozo , Phys. Rev.**D64**, 033004(2001), [arXiv:hep-ph/0212236].

[21] M. Sher and Y. Yuan, Phys. Rev. **D44**, 1461(1991).

[22] R. Martinez, D. A. Milanes, J.-Alexis Rodriguez, Phys. Rev. **D72**, (2005)035017, [arXiv:hep-ph/0502087].

[23] Y.F. Zhou, Y.L. Wu, Eur. Phys. J.**C27**:577-585(2003); Phys. Rev. **D64**, 115018(2001).

[24] U. Cotti, M. Pineda, G. Tavares-Velasco, [arXiv:hep-ph/0501162].